Electronic Supplementary Material (ESI) for Nanoscale.

Measuring Interactions of DNA with Nanoporous Protein Crystals by Atomic Force Microscopy

Supporting Information

Dafu Wang, [a,b] Julius D. Stuart, [c] Alec A. Jones, [d] Christopher D. Snow, [a,b,c,d] and Matt J. Kipper [a,b,d]*

a. *School of Advanced Materials Discovery, Colorado State University, 1617 Campus Delivery, Fort Collins, CO 80523 , USA*

b. *Department of Chemical and Biological Engineering, Colorado State University, 1370 Campus Delivery, Fort Collins, CO 80523, USA*

c. *Department of Chemistry, Colorado State University, 1872 Campus Delivery, Fort Collins, CO 80523, USA*

d. School of Biomedical Engineering, Colorado State University, 1301 Campus Delivery, Fort Collins, CO 80523, USA

* *Matthew.Kipper@colostate.edu*

2.1.1 CJ Crystals Growth

As described in previous work.[1] *Campylobacter jejuni* protein (CJ) was cloned into pSB3 expression vector. CJ expression was performed with BL21(DE3) *Escherichia coli* cells in Terrific broth. Induction was performed with 0.4 mM IPTG for 16 hours at 25 °C, followed by purification using immobilized metal affinity chromatography (IMAC). The target protein was then dialyzed into ammonium sulfate storage buffer (500 mM $(NH_4)_2SO_4$, 10 mM HEPES (4-(2-hydroxyethyl)-1-piperazineethanesulfonic acid), 10% glycerol, pH = 7.4). CJ protein was concentrated to 15 mg/mL, aliquoted and stored at -30 °C. Then, one tube (24 µL) of purified CJ protein (15 mg/mL) was thawed.[2-5] The samples were kept on ice at all times. In the reservoir of a plastic CrysChem sitting-drop crystallization plate, 340 µL of 4 M $(NH_4)_2SO_4$, 40 µL of 1 M bis-tris (pH = 6.5), and 20 µL of DI H_2O were mixed. Then, 1 µL of the reservoir solution was pipetted into the top drop of the plastic sitting-drop crystallization plate. Finally, a 1 µL aliquot of CJ protein solution was added by pipetting the protein solution directly on top of the drop of reservoir solution. Crystals typically grew to full size within 1 to 3 days.

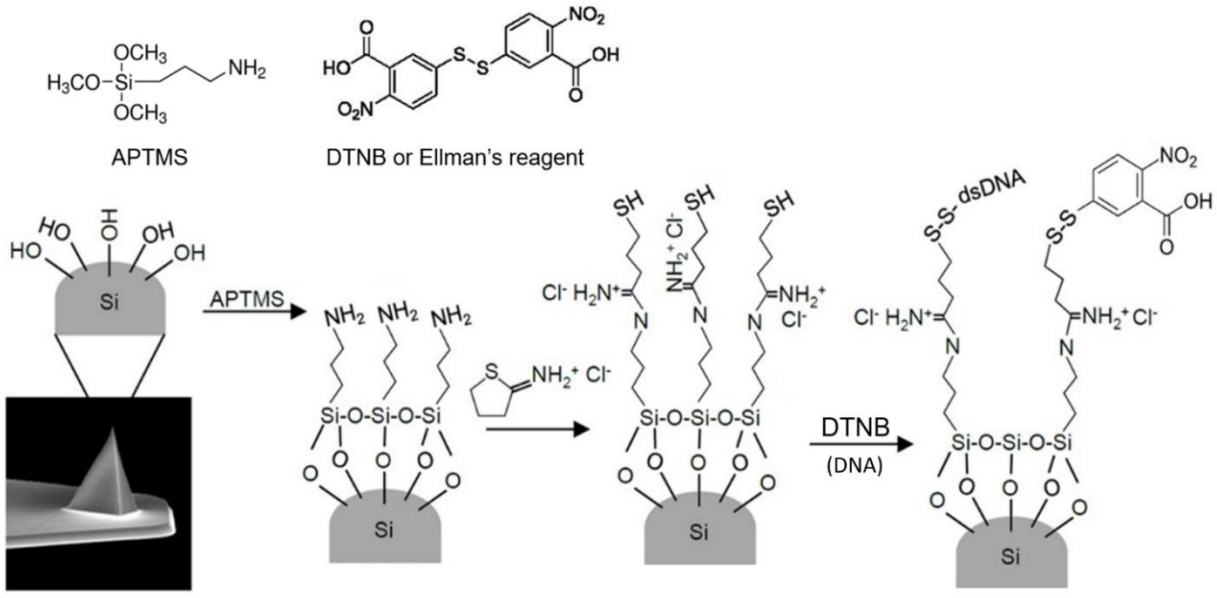

Fig. S1 Schematic illustration of intended AFM tip modification process

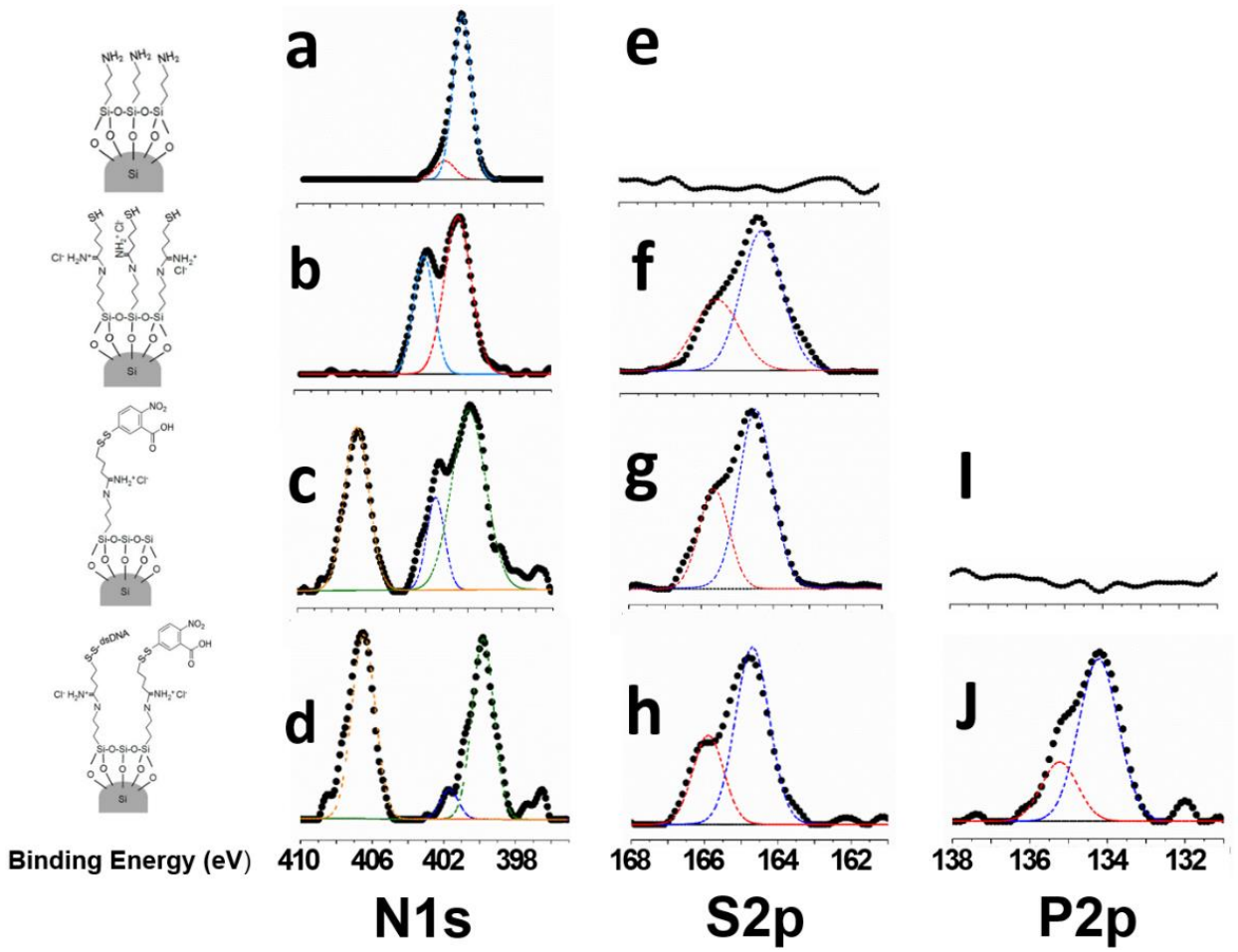

Fig. S2 High-resolution XPS spectra of ScanAsyst Fluid+ tips at different stages of modification in the regions of the N1s: (a) +APTMS (399.82 eV N-sp2 and 400.95 eV ammonium), (b) +2-iminothiolane (400.40 eV N-sp2 and 402.04 eV, ammonium), (c) +DTNB (399.84 eV N-sp2, 401.93 eV ammonium, and 406.55 eV nitrite O-N-O), (d) + 30mer DNA (399.84 eV pyridine N-sp2, 401.93 eV ammonium, and 406.55 eV nitrite O-N-O); and S2p: (f) +2-iminothiolane (thiols), (g) +DTNB (164.56 eV thiols), (h) + 30mer DNA (disulfide, thiols); and P2p: (j) +30mer DNA (O-P-O3 phosphate) envelopes confirmed that all of the samples were successfully modified at each step and able to bind DNA on the surface of AFM tips. (e) confirms that there is no sulfur signal prior to reaction with Traut's reagent, and (i) confirms that there is no detectable phosphorus prior to reaction with DNA.[6, 7]

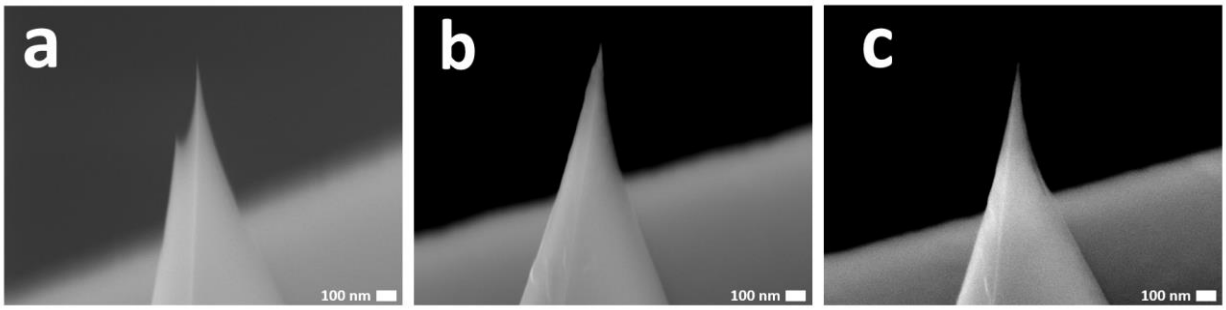

Fig. S3 The field emission scanning electron microscope imaging (FESEM, ×50000) of **(a)** unmodified ScanAsyst Fluid+ tip, **(b)** activated AFM tip without DNA, **(c)** modified AFM tip with 30mer DNA.

Table S1 Time scaled fluorescence intensity of the DNA inside and outside the crystal

Integrated Density/Area	Solution Fluorescence	Internal Crystal Fluorescence
Mean. (AU, time = 0)	980.896 / 979.894 / 974.104 / 966.443 / 972.423 ***(avg. mean = 974.752)***	989.490 / 989.684 / 997.717 / 983.990 / 977.960 ***(avg. mean = 987.769)***
Min. (AU, time = 0)	931 / 903 / 918 / ***753*** /922	957 / 940 / 945 / 955 / ***839***
Max. (AU, time = 0)	***1083*** / 1055 / 1029 / 1039 /1030	1015 / 1011 / ***1083*** / 1017 / 1029
Mean. (AU, time = end)	268.603 / 239.252 / 251.488 / 238.022 / 264.273 ***(avg. mean = 252.328)***	2852.836 / 2783.137 / 2944.677 / 2337.633 / 2797.874 ***(avg. mean = 2743.232)***
Min. (AU, time = end)	167 / 168 / ***151*** / 166 / 164	1979 / 2052 / 2059 / ***1602*** / 1755
Max. (AU, time = end)	***415*** / 370 / 414 / 389 / 393	3805 / 3558 / 3791 / 3400 / ***4065***

known: $V_{crystal} = 0.0237\ \mu L$
$V_{unit\ cell} = 1.413\times10^{-15}\ \mu L$
$V_{solution} = 100\ \mu L$
$[DNA]_{solution,\ time\ 0} = 50.0\ \mu M$

For dilute solutions, $I = k\varepsilon lc$ (I = intensity of fluorescence, k = constant number, ε = the molar attenuation coefficient, l = the optical path length, c = concentration), since ε, and l are known numbers, and $I \neq 0$ in this case, therefore as a result, $\frac{I_1}{I_2} = \frac{c_1}{c_2}$.

we can learn: $[DNA]_{avg.\ solution,\ time\ end} = 12.93\ \mu M$
$[DNA]_{avg.\ intra\text{-}crystal,\ time\ end} = 138.86\ \mu M$

This calculation of concentration ratio relies on the same linear relationship between concentration and fluorescence intensity that underlies a traditional fluorescence standards curve. Notably, it is likely not quantitatively accurate to attempt to use a traditional fluorescence standard curve to directly convert fluorescence intensity from the confocal microscope images into concentration due to inconstant optical effects (e.g. out of plane excitation)

Table. S2 (a) The min, 25th, 50th, 75th percentiles, and max of the adhesion energy for 20 pore center pixels and 20 wall pixels for each of the experiments detected in Fig. 2, **(b)** adhesion energy in the pores, normalized by the interacting pore area (adhesion energy divided by average area computed from the depth of penetration of the AFM tip into the pore) for 20 pore center pixels. and **(c)** detailed penetration depth data correspond to the Fig. 7 (d). The conditions labeled A-E here correspond to the conditions described in the Fig. 2.

(a) Adhesion energy (fJ)

	Pores					Walls				
Condition	**min**	**25 %-ile**	**50 %-ile**	**75 %-ile**	**max**	**min**	**25 %-ile**	**50 %-ile**	**75 %-ile**	**max**
A	4.55×10^{-3}	7.88×10^{-3}	9.23×10^{-3}	1.17×10^{-2}	1.57×10^{-2}	3.02×10^{-3}	3.52×10^{-3}	3.93×10^{-3}	4.29×10^{-3}	5.43×10^{-3}
B	3.50×10^{-2}	4.49×10^{-2}	5.02×10^{-2}	5.62×10^{-2}	8.08×10^{-2}	3.91×10^{-3}	1.16×10^{-2}	1.39×10^{-2}	1.69×10^{-2}	2.99×10^{-2}
C	1.54×10^{-2}	1.96×10^{-2}	2.31×10^{-2}	2.60×10^{-2}	3.16×10^{-2}	7.38×10^{-3}	8.78×10^{-3}	1.09×10^{-2}	1.35×10^{-2}	1.95×10^{-2}
D	3.69×10^{-3}	4.02×10^{-3}	4.50×10^{-3}	5.49×10^{-3}	9.55×10^{-3}	3.37×10^{-3}	3.84×10^{-3}	4.51×10^{-3}	5.00×10^{-3}	7.54×10^{-3}
E	1.15×10^{-2}	1.46×10^{-2}	1.70×10^{-2}	1.81×10^{-2}	2.59×10^{-2}	4.20×10^{-3}	5.63×10^{-3}	6.64×10^{-3}	8.56×10^{-3}	1.23×10^{-2}

(b) Normalized Adhesion energy (J m^{-2})

Condition	**25 %-ile**	**50 %-ile**	**75 %-ile**
A	1.46×10^{-2}	1.71×10^{-2}	2.16×10^{-2}
B	4.80×10^{-2}	5.37×10^{-2}	6.02×10^{-2}
C	4.86×10^{-2}	5.72×10^{-2}	6.42×10^{-2}
D	1.65×10^{-2}	1.85×10^{-2}	2.26×10^{-2}
E	6.14×10^{-2}	7.19×10^{-2}	7.63×10^{-2}

(c) Penetration Depth of Tip into Pores

Condition	**Penetration Depth (nm)**
A	13.2 ± 4.1 (n = 579)
B	22.9 ± 7.3 (n = 335)
C	9.9 ± 4.4 (n = 164)
D	6.0 ± 2.4 (n = 324)
E	5.8 ± 2.4 (n = 173)

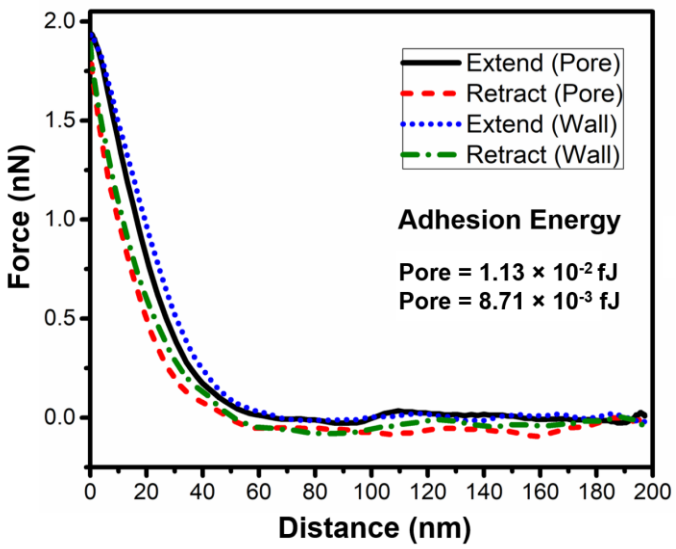

Fig. S4 One randomly selected set of F-D curves, using an inactivated AFM tip on a DNA loaded crystal, obtained from both pore and wall pixels.

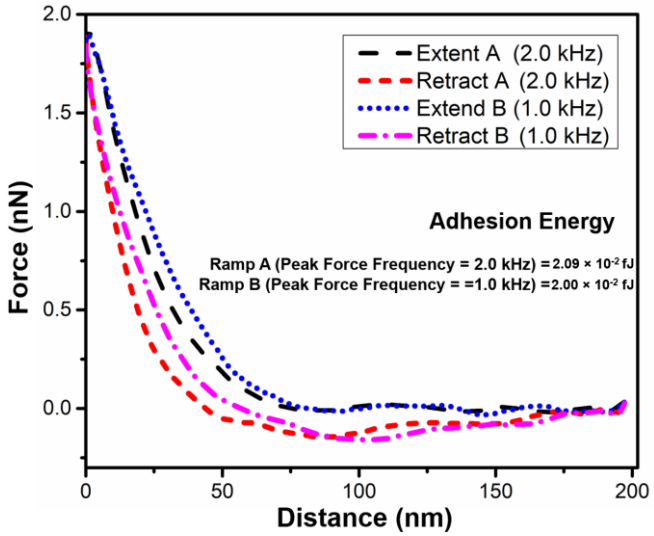

Fig. S5 Two sets of ramping F-D curves in different peak force frequency, respectively 1.0 kHz and 2.0 kHz, using an activated AFM tip on a DNA loaded crystal. The curves were from the same randomly selected pixel, in addition to the peak force frequency, all other imaging parameters were the same.

Table S3 Selected imaging parameters related to the Fig. S2

Feedback		**Peak Force Tapping Control**	
Peak Force Setpoint	2.0 nN	Peak Force Amplitude	100 nm
		Peak Force Frequency	**(A)** 2.0 kHz / **(B)** 1.0 kHz

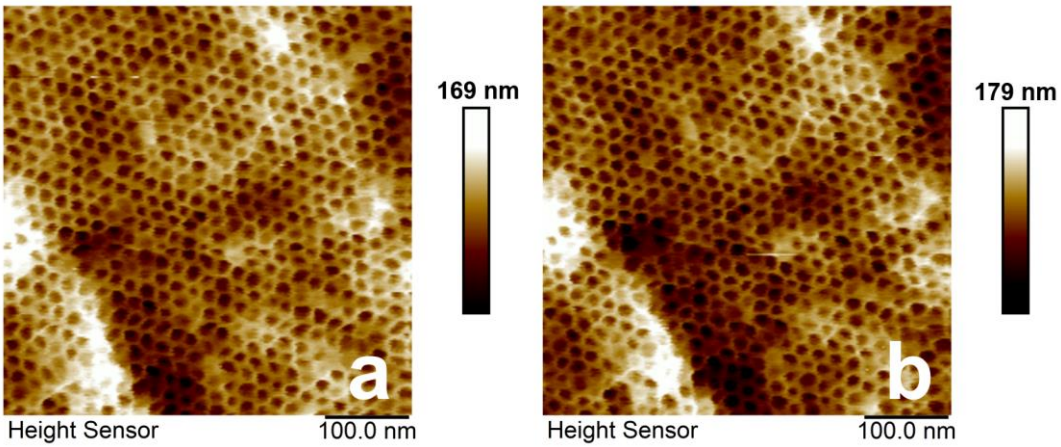

Fig. S6 AFM images of a crystal loaded with DNA imaged using an activated AFM tip in a scan rate of **(a)** 1.0 Hz and **(b)** 2.0 Hz, respectively. In addition to the scan rate, all other imaging parameters were the same.

Table S4 Selected imaging parameters related to the Fig. S6 (a-b)

Scan		**Feedback**		**Peak Force Tapping Control**	
Scan Size	500 × 500 nm	Peak Force Setpoint	2.0 nN	Peak Force Amplitude	100 nm
Scan Rate	**(a)** 1.0 / **(b)** 2.0 Hz			Peak Force Frequency	1.0 kHz
Scanning Lines	512				

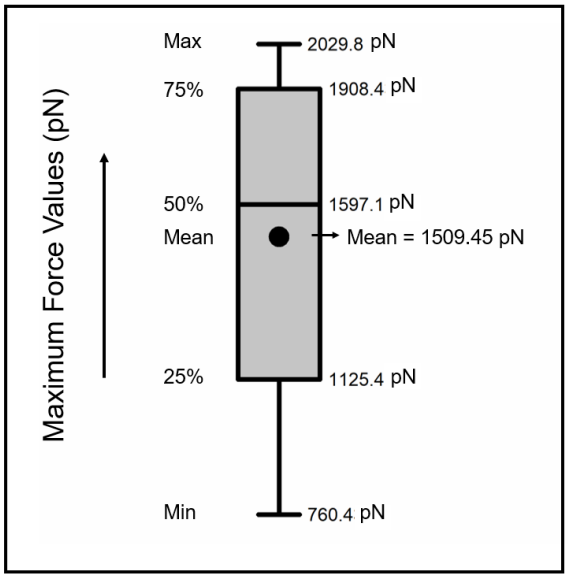

Fig. S7 Box plot (min, 25th, 50th, 75th percentiles, mean, and max) for the distribution of maximum force values between DNA and protein crystals, in the pore areas, under scenario B and E of Fig. 2 and Fig. 9.

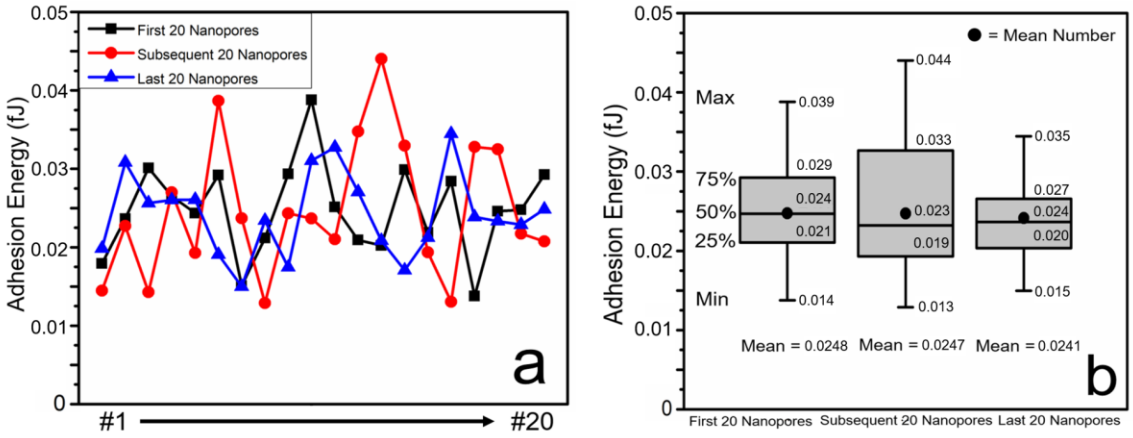

Fig. S8 (a) Line charts and **(b)** box plot (min, 25th, 50th, 75th percentiles, mean, and max) for the pore area adhesion energy of the first, the subsequent, and the last 20 nanopores, during one AFM imaging, from activated AFM tips with DNA loaded crystal.

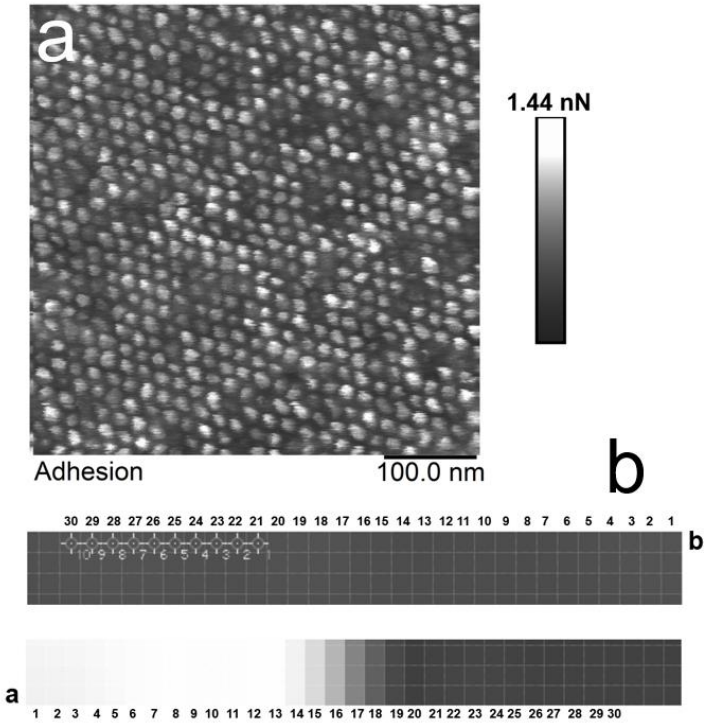

Fig. S9 (a) an adhesion energy map for activated AFM tip with DNA loaded protein crystal, **(b)** the very first 30 scanned pixels (from a1to a30) of imaging, and after 16 minutes, the very last 30 scanned pixels (from b30 to b1) of imaging, from the adhesion energy map Fig. S9 (a). The dark pixels locate at the wall areas while the bright pixels locate at the pore areas. Along with the corresponding grayscale data, the results indicate that during that 16 mins, the ability of attachment for activated tips was stable and consistent.

Table S5 The grayscale of very first 30 scanned pixels (from a1to a30) of imaging, and after 16 minutes, the very last 30 scanned pixels (from b30 to b1) of corresponding to the Fig. S9 (b), from the adhesion energy map Fig. S9 (a).

Pixel	Grayscale (K) 16-bit (0-32768)	Pixel	Grayscale (K) 16-bit (0-32768)
a1	30435	**b1**	8120
a2	30600	**b2**	8120
a3	30765	**b3**	8007
a4	31262	**b4**	7780
a5	31762	**b5**	7555
a6	32263	**b6**	7442
a7	32432	**b7**	7332
a8	32600	**b8**	7220
a9	32432	**b9**	7332
a10	32432	**b10**	7332
a11	32432	**b11**	7332
a12	32600	**b12**	7332
a13	32600	**b13**	7220
a14	30600	**b14**	7332
a15	26708	**b15**	7442
a16	21010	**b16**	7555
a17	14086	**b17**	7893
a18	9526	**b18**	8007
a19	6890	**b19**	8007
a20	5820	**b20**	7893
a21	6242	**b21**	7780
a22	6455	**b22**	7666
a23	6564	**b23**	7666
a24	6564	**b24**	7666
a25	6349	**b25**	7893
a26	6135	**b26**	8120
a27	6135	**b27**	8236
a28	6135	**b28**	8236
a29	6135	**b29**	8236
a30	6135	**b30**	8120

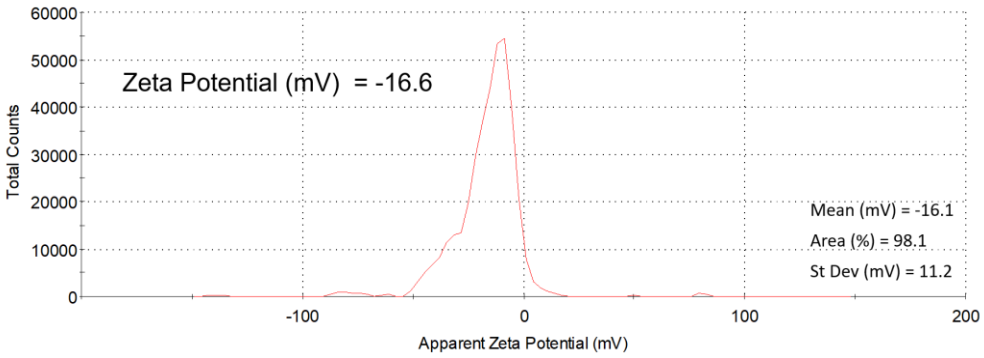

Fig. S10 Zeta potential distribution on the surface of crosslinked CJ protein crystals

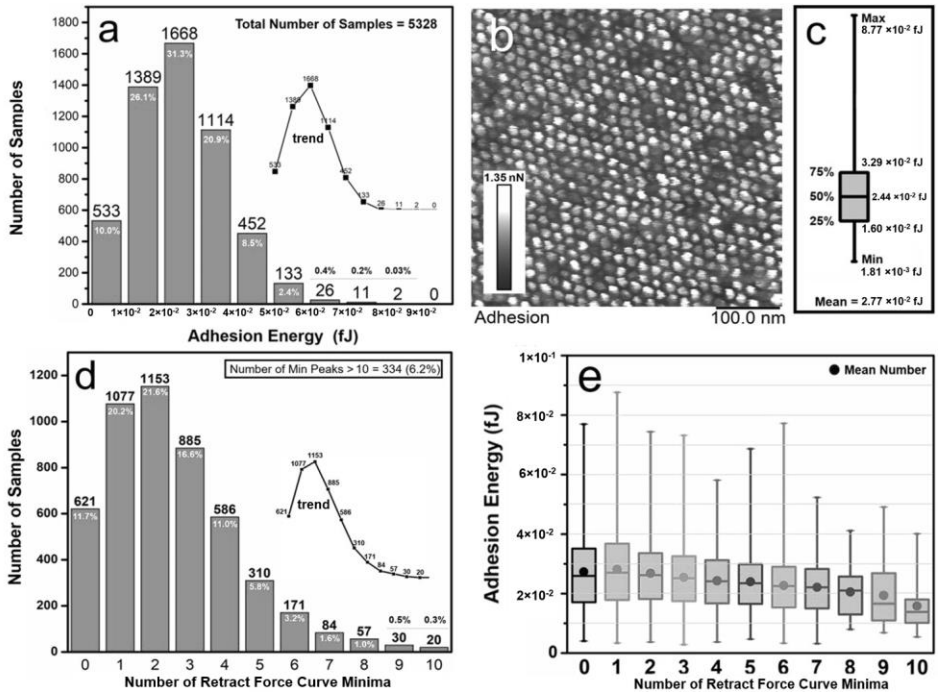

Fig. S11 (a) Distribution of adhesion energy ranges, **(b)** a map of adhesion energy corresponding to Fig. 5 (a), along with the corresponding grayscale data for the very initial and very last scanned pixels (Supporting Information Fig. S9 and Table S5), the results can also indicate that during that 16 mins of imaging, the ability of attachment for activated AFM tips was stable and consistent, and **(c)** box plot (min, 25th, 50th, 75th percentiles, and max) of the adhesion energy, for 5328 pore center pixels (from 5328 individual pores) with activated AFM tip, on the crystal loaded with DNA, and **(d)** distribution of numbers of minimum peak(s) (as labeled on Fig. 6 (a)) on each individual retract force curve. **(e)** box plot (min, 25th, 50th, 75th percentiles, mean, and max) of the adhesion energy distribution, corresponding to the number of minimum peak(s) among retract force curves in Fig. 7 (d).

Reference

1. McPherson, A., A. Malkin, and Y. G, *Atomic force microscopy in the study of macromolecular crystal growth.* Annu. Rev. Biophys., 2000. **29**(1): p. 361-410.
2. Ilari, A. and C. Savino, *A practical approach to protein crystallography,* in *Bioinformatics*. 2017, Springer. p. 47-78.
3. Wlodawer, A., et al., *Protein crystallography for aspiring crystallographers or how to avoid pitfalls and traps in macromolecular structure determination.* FEBS J., 2013. **280**(22): p. 5705-5736.
4. Wlodawer, A., et al., *Protein crystallography for non-crystallographers, or how to get the best (but not more) from published macromolecular structures.* FEBS J., 2008. **275**(1): p. 1-21.
5. Kowalski, A.E., et al., *Gold nanoparticle capture within protein crystal scaffolds.* Nanoscale, 2016. **8**(25): p. 12693-12696.
6. Crist, B.V. and D.B. Crisst, *Handbook of monochromatic XPS spectra*. Vol. 1. 2000: Wiley New York.
7. Crist, B.V., *A review of XPS data-banks.* XPS Reports, 2007. **1**(1).